Journal of Power Sources 269 (2014) 616–620

Contents lists available at ScienceDirect

Journal of Power Sources

journal homepage: www.elsevier.com/locate/jpowsour

Short communication

# Corrosion of stainless steel battery components by bis(fluorosulfonyl) imide based ionic liquid electrolytes

Tyler Evans [a], Jarred Olson [b], Vinay Bhat [b], Se-Hee Lee [a, *]

[a] Department of Mechanical Engineering, University of Colorado, Boulder, CO 80309, USA
[b] Boulder Ionics Corporation, Arvada, CO 80007, USA

## HIGHLIGHTS

- $PYR_{13}FSI$ + LiFSI based electrolytes corrode SS battery components at high voltages.
- SS corrosion by $PYR_{13}FSI$ + LiFSI is exacerbated by addition of organic solvent.
- SS oxidation prevents cycling of high-voltage electrodes in $PYR_{13}FSI$ solutions.

## ARTICLE INFO

*Article history:*
Received 12 May 2014
Received in revised form
6 July 2014
Accepted 9 July 2014
Available online 17 July 2014

*Keywords:*
Ionic liquids
$PYR_{13}FSI$
Stainless steel
Corrosion

## ABSTRACT

While the anodic behavior of aluminum foil current collectors in imide-based room temperature ionic liquids (RTILs) is relatively well understood, interactions between such RTILs and other passive battery components have not been studied extensively. This study presents the solvent and potential dependent oxidation of SS316 coin-cell components in the *N*-methyl-*N*-propyl-pyrrolidinium bis(fluorosulfonyl) imide ($PYR_{13}FSI$) RTIL. While this phenomenon prohibits high-voltage cycling of $Li(Ni_{1/3}Mn_{1/3}Co_{1/3})O_2$ cathodes in SS316 coin-type cells, Al-clad cell components or alternative cell configurations can be utilized to avoid SS316 oxidation-induced cell failure.



## 1. Introduction

Room temperature ionic liquid (RTIL) based electrolyte solutions represent an attractive alternative to conventional carbonate electrolytes for lithium-ion batteries (LIBs) due to their potential to mitigate safety concerns related to the volatility and flammability of commercialized organic electrolytes. Much work has been dedicated to developing RTIL electrolytes that are compatible with commercially attractive electrode materials and capable of high electrochemical performance [1,2]. Due to constraints associated with solution viscosity, which dictates ionic conductivity in RTILs via the Walden Rule, and compatibility with low voltage negative electrode materials such as graphite, the most widely studied RTILs are those which contain pyrrolidinium cations and sulfonyl imide anions, namely bis(trifluoromethanesulfonyl)imide (TFSI) and bis(fluorosulfonyl)imide (FSI) [3]. In addition to understanding the electrochemical performance and interactions between RTIL-based electrolytes and electrode materials, it is imperative to develop an understanding of the compatibility of RTILs with a battery's structural components.

Unfortunately, the sulfonyl imide anion has been found to induce severe corrosion of the aluminum current collector used on the positive electrode of LIBs. This oxidation process is dependent on solvent content and electrolyte composition and has been documented in electrochemical cells containing the TFSI anion [4–7] and the FSI anion [3,8]. The oxidative dissolution of aluminum occurs through a mechanism initiated by sulfonyl imide anion attack of the native oxide layer on the surface of the aluminum current collector ($Al_2O_3$) at high potentials (>4.2 V vs. $Li/Li^+$). The ions subsequently form Al-imide complexes, e.g. $Al(TFSI)_3$, which are solvated by the electrolyte solution, thereby leaving large pits in the aluminum sheet and introducing metal ions into the electrolyte [3,6,7]. While this mechanism is well understood, the possibility of an interaction between the RTIL and other battery components has largely been disregarded.

* Corresponding author. Department of Mechanical Engineering, ECME 275, 427 UCB, Boulder, CO 80309, USA. Tel.: +1 303 492 7889; fax: +1 303 492 3498.
*E-mail address:* sehee.lee@colorado.edu (S.-H. Lee).

http://dx.doi.org/10.1016/j.jpowsour.2014.07.047
0378-7753/

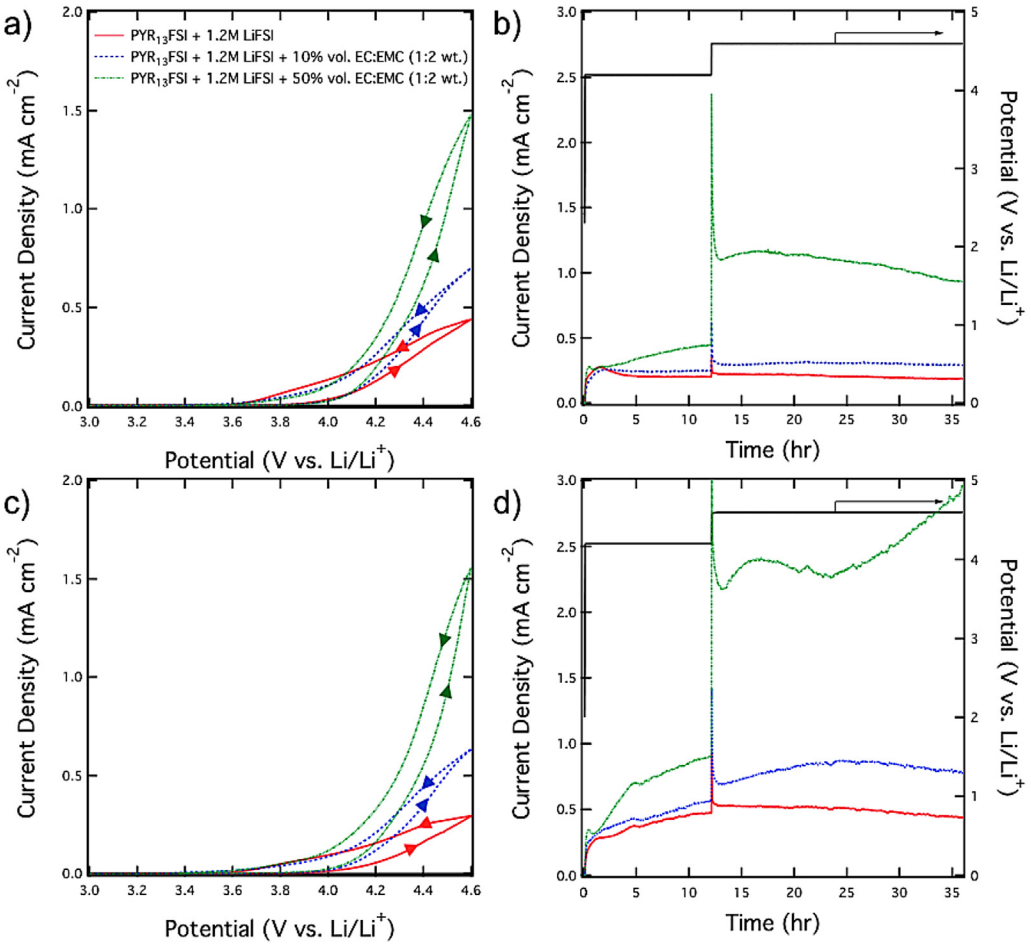


**Fig. 1.** Cyclic voltammograms and chronoamperograms of pure aluminum foil (a, b) and SS316 foil (c, d) in SS316 2032 coin-type cells containing $PYR_{13}FSI$ + 1.2 M LiFSI and various volumetric amounts of organic co-solvent.

In this study, we demonstrate the voltage and solvent dependent oxidation of Grade 316 stainless steel (SS316) in electrochemical cells containing the *N*-methyl-*N*-propyl-pyrrolidinium bis(fluorosulfonyl)imide ($PYR_{13}FSI$) RTIL with 1.2 M dissolved LiFSI salt. While steel corrosion and electropolishing by RTILs are not new phenomena [9–12], this is, to our knowledge, the first study describing RTIL-induced steel oxidation in LIBs. SS316 coin-type cells are commonly used to test electrode and electrolyte materials for LIBs, thus it is essential to generate an awareness of the interactions between RTIL electrolytes and SS316 during electrochemical cycling. As a counter measure to eliminate such interactions, alternative testing apparatus such as Al-clad cathode casings can be utilized.

## 2. Experimental

$PYR_{13}FSI$ was the ionic liquid selected for this study. Ionic liquid solutions were provided by Boulder Ionics Corporation (U.S.A.) and contained less than 20 ppm (w/w) of moisture and less than 10 ppm (w/w) of halide and metal-ion impurities. A 1:2 weight ratio of ethylene carbonate and ethyl methyl carbonate (EC:EMC; BASF) was utilized as organic solvent and added to the $PYR_{13}FSI$ electrolytes in 10 vol.% EC:EMC and 50 vol.% EC:EMC mixtures. LiFSI (1.2 M), provided by Boulder Ionics Corp., was added as the lithium salt subsequent to mixing the electrolyte solvents.

To evaluate the corrosion behavior, high-grade aluminum foil (ESPI Metals; 25 μm thick; >99.5% purity) and SS316 foil (MTI Corp.; 0.1 mm thick) were punched into 1.27 cm diameter disks, rinsed in dimethyl carbonate (DMC) and dried at 120 °C in a vacuum oven for 12 h before testing. Corrosion cells contained an aluminum or SS316 disc working electrode and lithium foil counter electrode and were assembled in 2032 coin-type cells (Hohsen). Cyclic voltammetry (CV; Solartron 1280C), chronoamperometry (Arbin BT2000), and low vacuum scanning electron microscopy (LVSEM; JEOL SEM 6480LV) were utilized to characterize oxidative currents and morphological changes associated with the corrosion process. Cyclic voltammetry was performed on corrosion cells by cycling potential between 3.0 V and 4.6 V vs. $Li/Li^+$ at a scan rate of 1 mV $s^{-1}$. During chronoamperometry, the working electrode potential was ramped from open circuit voltage (OCV) to 4.2 V vs. $Li/Li^+$ at a sweep rate of 100 mV $s^{-1}$ and held for 12 h; the potential was then ramped from 4.2 V to 4.6 V vs. $Li/Li^+$ at a sweep rate of 100 mV $s^{-1}$ and held for 24 h. Infrared (IR) spectroscopy was used to characterize possible changes in solution chemistry induced by SS316 oxidation. Energy-dispersive X-ray spectroscopy (EDX; JEOL SEM 6480LV) was used to characterize changes in SS316 elemental composition after corrosion by $PYR_{13}FSI$-based electrolyte.

Composite electrodes were fabricated using $Li(Ni_{1/3}Mn_{1/3}Co_{1/3})O_2$ powder active material (Johnson Controls), acetylene black (AB; Afla Aesar) as a conductive additive, and polyvinyldene fluoride (PVDF; Kynar) binder in a weight ratio of (85:7.5:7.5). The composite was mechanically cast onto a clean, high-grade aluminum foil current collector, dried, and calendared to 75% of its initial thickness to ensure adequate electrical contact. Potentiogalvanostatic cycling (Arbin BT2000) experiments utilized $Li(Ni_{1/3}Mn_{1/3}Co_{1/3})O_2$ positive electrodes and lithium foil negative

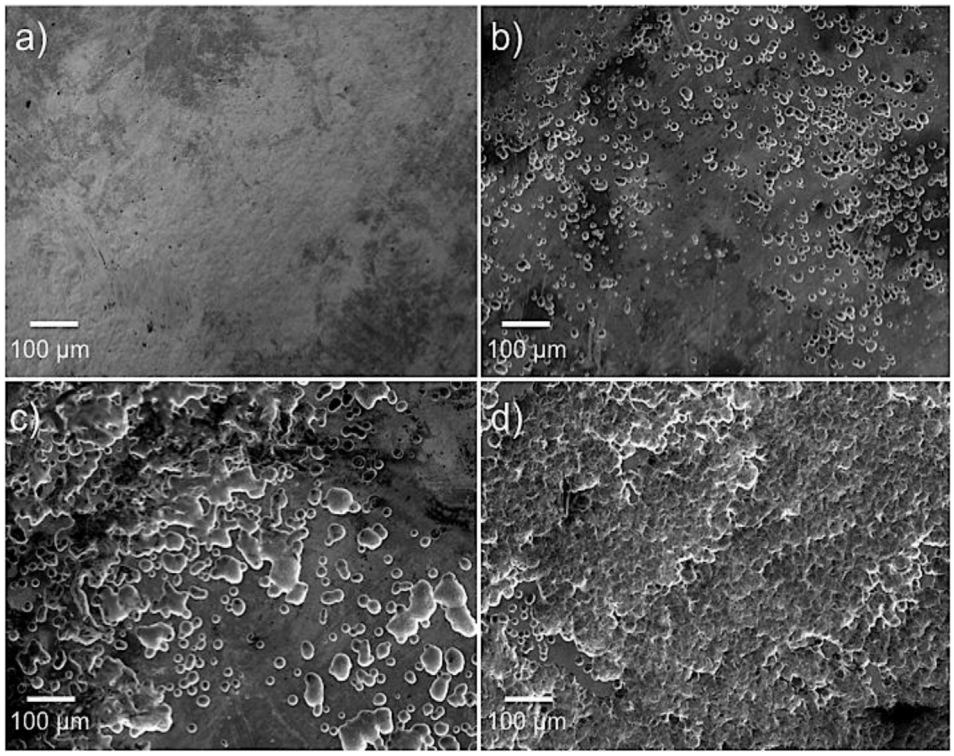


**Fig. 2.** SEM micrographs of pristine SS316 foil (a) and SS316 foil after extended charging at 4.6 V vs. $Li/Li^+$ in $PYR_{13}FSI$ + 1.2 M LiFSI solutions containing 0% vol. organic solvent (b), 10% organic solvent (c), and 50% organic solvent (d).

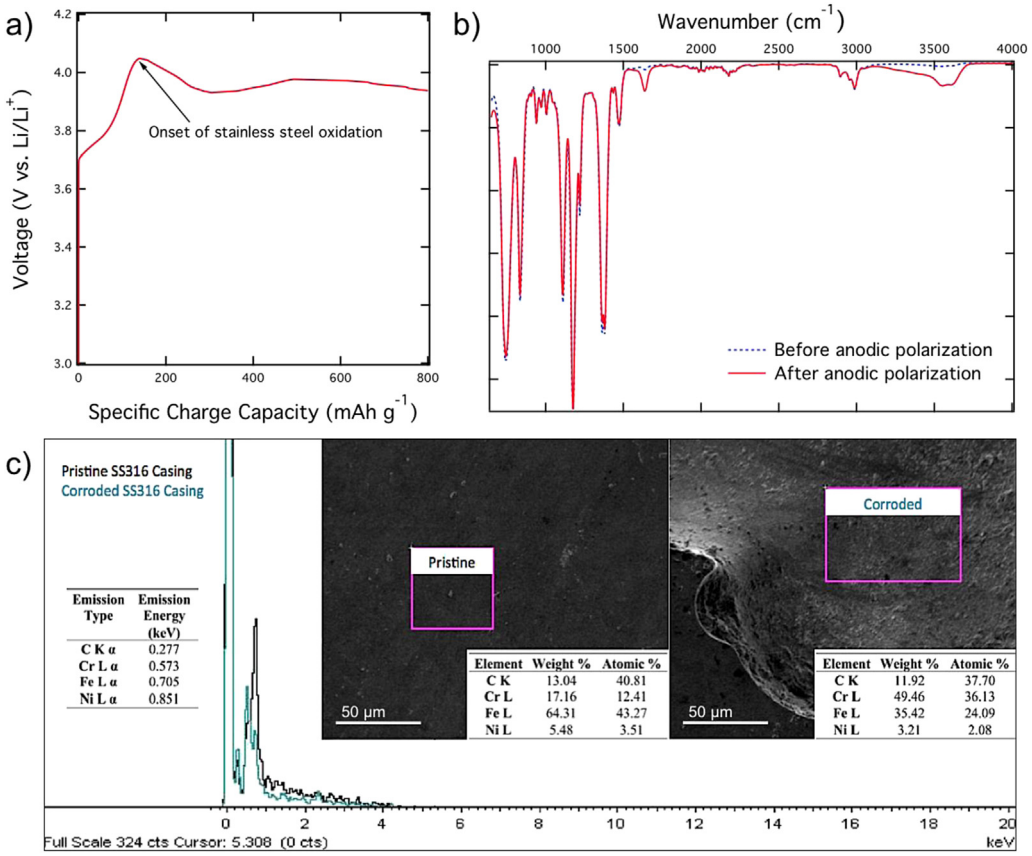


**Fig. 3.** First charge voltage profile of a $Li(Ni_{1/3}Mn_{1/3}Co_{1/3})O_2$ half-cell in $PYR_{13}FSI$ + 1.2 M LiFSI electrolyte in a SS316 2032 coin-type cell (a), IR spectra of the $PYR_{13}FSI$ + 1.2 M LiFSI solution before and after extended charging at 4.6 V vs. $Li/Li^+$ (b), and EDX spectra of the surfaces of pristine SS316 and a pit formed by exposure of SS316 to extended charging at 4.6 V vs. $Li/Li^+$ in $PYR_{13}FSI$ +1.2 M LiFSI solution, including compositional analysis of both samples (c).

electrodes assembled in 2032 coin-type cells (Hohsen). All cells used in this study contained glass microfibre filters (Whatman; grade GF/F) wetted with the IL-EC:EMC solutions as the electrolyte separator layer.

## 3. Results and discussion

Stainless steel casing oxidation was originally observed during a set of experiments designed to investigate the solvent dependent aluminum corrosion in $PYR_{13}FSI$ + LiFSI based electrolytes. High-grade aluminum foil discs were loaded into SS316 2032 coin-type cells with mixtures of $PYR_{13}FSI$ + 1.2 M LiFSI and various volumetric amounts of organic solvent as electrolyte solutions. Fig. 1 presents initial CV cycles and chronoamperometric data for all corrosion cells tested in this study. The solvent dependent oxidative current densities exhibited in aluminum corrosion cells increased with higher volumes of organic content in accordance with data from previous studies [4–7]. However, the current densities observed in CV and extended charging at both 4.2 V vs. $Li/Li^+$ and 4.6 V vs. $Li/Li^+$ were higher than expected, with initial CV scans showing irreversible oxidative current densities approaching 1.5 mA $cm^{-2}$ and current densities of approximately 1 mA $cm^{-2}$ observed during chronoamperometry in cells containing 50% vol. organic solvent. Corrosion cells containing pure RTIL electrolyte showed irreversible oxidative current densities approaching 500 μA $cm^{-2}$ during the initial CV scan and current densities of about 250 μA $cm^{-2}$ during chronoamperometry. A study by Cho et al. demonstrates that pure FSI-based RTILs show initial scan current density amplitudes of <50 μA $cm^{-2}$ during CV between 3.0 and 5.5 V vs. $Li/Li^+$ [3]. Because of the $PYR_{13}FSI$ RTIL's large electrochemical stability window (7.31 V), current densities were not attributed to electrolyte decomposition.

CV and chronoamperometry were performed on corrosion cells containing SS316 foil working electrodes in order to investigate the possible oxidation of the stainless steel cell components (Fig. 1c and d). CV results were similar to those obtained during the same tests using pure aluminum foil working electrodes, while the oxidative currents observed during extended charging at both 4.2 V vs. $Li/Li^+$ and 4.6 V vs. $Li/Li^+$ were about twice as high as those in the aluminum corrosion cell experiments. Chronoamperometry of SS316 foil in the FSI-based electrolyte containing 50% vol. organic solvent showed an oxidative current density that continually increased over 12 h during exposure to 4.6 V vs. $Li/Li^+$. The data obtained from corrosion cells made in SS316 coin-type cells show obvious contrast to data obtained under the same experimental conditions in Al-clad 2032 casings with pure aluminum foil working electrodes [8]. This result leads us to believe that the oxidative current densities observed in the aluminum corrosion cell experiments were significantly influenced by a parasitic interaction between the RTIL and SS316.

LVSEM imaging of SS316 working electrodes was performed subsequent to the chronoamperometry experiments to analyze morphological effects associated with the observed oxidative currents. High-resolution SEM micrographs, provided in Fig. 2, reveal pitting corrosion on each sample, with the size and density of the pits increasing with organic co-solvent content in the corrosion cells. The corrosion cell with 50% vol. organic solvent shows a network of pits covering the entire surface of the SS316 foil.

The stainless steel corrosion phenomenon was substantiated by attempts to cycle $Li(Ni_{1/3}Mn_{1/3}Co_{1/3})O_2$ half-cells in SS316 2032 coin-type cells containing pure $PYR_{13}FSI$ + 1.2 M LiFSI electrolyte. The $Li(Ni_{1/3}Mn_{1/3}Co_{1/3})O_2$ electrochemical cycling voltage profile is shown in Fig. 3a. During initial galvanostatic charge at a current density of 50 μA $cm^{-2}$, corresponding to a rate of C/10, cells were unable to charge to the target voltage of 4.2 V vs. $Li/Li^+$. The potential peaked at ~4.05 V vs. $Li/Li^+$, which corresponds to the onset of SS316 oxidation observed during CV. The cell potential remained below 4.05 V vs. $Li/Li^+$, suggesting that the 50 μA $cm^{-2}$ current density was drawn from the oxidation of species present in the SS316 cell casing and possibly the aluminum current collector rather than delithiation of the $Li(Ni_{1/3}Mn_{1/3}Co_{1/3})O_2$ electrode.

IR spectroscopy was performed on the FSI-based electrolyte before and after extended charging of an SS316 sample in a cell containing $PYR_{13}FSI$ + 1.2 M LiFSI solution, and results are presented in Fig. 3b. The IR spectra reveal that the corrosion process does not affect the bonding chemistry of the $PYR_{13}FSI$ RTIL. While an −OH stretch at ~3500 $cm^{-1}$ and a −C═O stretch at ~1600 $cm^{-1}$ are attributed to moisture and $CO_2$ impurities introduced by the flow IR system in the post-corrosion sample, respectively, the electrolyte's IR "fingerprint" (500–1500 $cm^{-1}$) remains unchanged, suggesting that the RTIL maintains the same chemical structure and bonding environment while solvating cations pulled from the stainless steel.

Using EDX analysis, the elemental composition of the SS316 surface was observed before oxidation and compared to the surface composition of a pit formed during extended charging in $PYR_{13}FSI$ +1.2 M LiFSI solution. Fig. 3c provides EDX analysis of pristine and corroded SS316. The corroded sample shows significantly lower iron and nickel content, suggesting the selective oxidation and solvation of iron and nickel by the RTIL electrolyte during exposure to high potentials.

The combination of CV, chronoamperometry, SEM, IR, and EDX data leads us to believe that the solvent and potential dependent corrosion of SS316 in electrochemical cells containing $PYR_{13}FSI$ + 1.2 M LiFSI occurs by a mechanism similar to the aluminum oxidative dissolution previously observed in RTIL electrolytes [3,6–8]. It is suggested that oxidized ions in the SS316 casing are solvated by the electrolyte solution, leaving pits in the metal surface and limiting battery performance. While SS316 corrosion prohibits electrochemical cycling under high voltage conditions, steel corrosion can be avoided by utilizing aluminum-clad cell components. $Li(Ni_{1/3}Mn_{1/3}Co_{1/3})O_2$ half-cells containing the $PYR_{13}FSI$ + 1.2 M LiFSI electrolyte are capable of extended cycling between 3.0 and 4.2 V vs. $Li/Li^+$ in Al-clad 2032 coin-type cells [8]. It is imperative that future study of RTILs for application in lithium-ion batteries considers the stainless steel oxidation phenomenon.

## 4. Conclusions

This work demonstrates the voltage and solvent dependent oxidation of SS316 coin-cell components during electrochemical cycling of high-voltage electrode materials in $PYR_{13}FSI$ + 1.2 M LiFSI electrolytes. SS316 oxidation likely occurs via a mechanism similar to the well-documented aluminum oxidative dissolution previously described in imide-based RTILs. While steel corrosion causes cell failure, the effect can be avoided by removing SS316 components from the cell by using materials such Al-clad cathode cups.

## Acknowledgments

Funding for this work comes from Boulder Ionics Corporation through the Membrane Science, Engineering and Technology (MAST) Center at CU-Boulder, an NSF Industry–University Cooperative Research Center. This material is based upon work supported by the National Science Foundation under Grant No. IIP-1152040. Any opinions, findings, and conclusions or recommendations expressed in this material are those of the author(s) and do not necessarily reflect the views of the National Science Foundation.

## References

[1] A. Lewandowski, A. Świderska-Mocek, J. Power Sources 194 (2009) 601.
[2] M.A. Navarra, MRS Bull. 38 (2013) 548.
[3] E. Cho, J. Mun, O.B. Chae, O.M. Kwon, H.-T. Kim, J.H. Ryu, Y.G. Kim, S.M. Oh, Electrochem. Commun. 22 (2012) 1.
[4] L.J. Krause, W. Lamanna, J. Summerfield, M. Engle, G. Korba, R. Loch, R. Atanasoski, J. Power Sources 68 (1997) 2.
[5] M. Morita, T. Shibata, N. Yoshimoto, M. Ishikawa, Electrochim. Acta 47 (2002) 2787.
[6] R.S. Kühnel, M. Lübke, M. Winter, S. Passerini, A. Balducci, J. Power Sources 214 (2012) 178.
[7] E. Krämer, S. Passerini, M. Winter, ECS Electrochem. Lett. 1 (2012) C9.
[8] T. Evans, J. Olson, V. Bhat, S.-H. Lee, J. Power Sources 265 (2014) 132.
[9] M.F. Arenas, R.G. Reddy, J. Min. Metall. 39B (2003) 81.
[10] M. Uerdingen, C. Treber, M. Balser, G. Schmitt, C. Werner, Green Chem. 7 (2005) 321.
[11] A.P. Abbott, G. Capper, K.J. McKenzie, A. Glidle, K.S. Ryder, Phys. Chem. Chem. Phys. 8 (2006) 4214.
[12] A.P. Abott, G. Capper, K.H. McKenzie, K.S. Ryder, Electrochim. Acta 51 (2006) 4420.